

Modeling of Frequency Characteristics of Automatic Control Systems of Peltier Thermoelectric Modules

Vasilyev G. S.¹, Kuzichkin O. R.², Surzhik D. I.³ and Podmasteryev K.V.⁴

¹*Phd., Associate Professor Gleb S. Vasilyev*

¹*D.Sc. in Engineering, Professor Oleg R. Kuzichkin*

^{1,2}*Phd., Associate Professor Dmitry I. Surzhik*

⁴*D.Sc. in Engineering, Professor Podmasteryev K.V.*

¹*Belgorod State Research University, Russia*

²*Vladimir State University named after Alexander G. and Nikolai G. Stoletovs, Russia*

⁴*Oryol state University named after I. S. Turgenev, Russia*

Abstract

The numerous advantages of thermoelectric systems based on Peltier modules (TEM) determine the high prospects for their applications when traditional compressor cooling systems are ineffective (radioelectronic, aerocomic, medical, industrial equipment, etc.). It is shown that to improve the characteristics of climate control systems based on TEM, it is promising to analyze the frequency characteristics of the system for influences applied to various points of the system. A block diagram of a two-channel climate control system based on TEM has been developed according to the principle of combined control, which allows to achieve both a high speed of temperature transients and high interference suppression. Based on the transfer functions for three impacts, the amplitude-frequency and phase-frequency characteristics of the system of different orders and with different inertial properties are obtained. Analytical expressions and graphs of the frequency characteristics of the system for various types and orders of the filter in the control circuit are shown. The results of the analysis can be used to optimize the dynamic properties of the system under the influence of interference with different spectral characteristics.

Keywords: thermoelectrics, Peltier effect, thermoelectric modules, transfer function, frequency response.

Introduction

Recently, there has been a great interest in thermoelectric energy conversion, and the production of thermoelectric equipment is actively developing all over the world. Thus, in recent years, the average increase in the global production of thermoelectric modules (TEM) and thermoelectric devices for various purposes is about 14-15% [1-3], and the projected growth until 2027 is 11.7 % [4].

Thermoelectric energy converters have many advantages over traditional compressor cooling systems. In particular, they allow to provide not only cooling, but also heating, by simply switching the polarity of the applied voltage. Due to the absence of moving parts, they have high reliability and low sensitivity to mechanical loads, which allows them to be used on mobile objects for radio-electronic, aerospace, medical, industrial and household appliances [5-13]. To achieve a high accuracy of temperature control and the possibility of temperature control by changing the power supply current, it is necessary to develop an effective TEM control system [14-15].

Liu et al. [16] presented theoretical and experimental studies of a new solar thermoelectric air conditioner with hot water supply. It follows from this study that the heat transfer coefficient of the system can be about 2.59 in the cooling mode and 3.01 in the heating mode. Yazeed-Alomair et al [17] studied the use of thermoelectric modules for cooling water via a solar-thermoelectric liquid cooling system consisting of an array of six thermoelectric modules.

Aboelmaaref et al. [18] determined the best standards of the solar energy with technological cooling and air conditioning systems, such as thermoelectric and thermoelectronic, for use in large-scale facilities, since its productivity has reached at least 30%, which is very promising, primarily in hot climate. A thermoelectric air conditioner was designed and built, which can be used for personal cooling and heating. Four fuel and energy systems were used to achieve cooling using a DC power source via an external power source. According to the results of the assessment, the thermoelectric power was 430 W and cooling capacity 2.6. The efficiency of thermoelectric and thermal emission characteristics can be improved by optimizing heat exchange and improving the configuration of products in thermoelectric and thermal emission systems, which makes it easier to use thermoelectric and thermal emission systems for their use in refrigeration and air conditioning in remote areas.

Despite the wide scope of application of TEM-based systems and their obvious advantages, there is currently a limited number of works devoted to the study of their quality indicators. Thus, in [19-21], the identification of thermoelectric systems is performed based on the analysis of transient processes. The possibility of diagnosing TEM malfunctions based on the analysis of their dynamic characteristics is also investigated [22-23]. The analysis and synthesis of thermoelectric systems by the methods of the theory of automatic control is carried out [24-26]. Thus, in the work [26], a method for synthesizing a temperature controller was developed. An abrupt and trapezoidal temperature profile is considered as an input effect. The calculation of the temperature indicator is based on the application of the motion separation method. The results of numerical simulation of the temperature control system are presented. The

proposed temperature control system for the Peltier element has high accuracy, which makes it possible to use in the thermogenerators on biophysical objects.

To improve the characteristics of climate control systems based on TEM, it is promising to analyze the frequency characteristics of the system for impacts applied to various units. The results of the analysis can be used to optimize the dynamic properties of the system under the interference with different spectral characteristics.

The aim of the work is to develop and apply a methodology for modeling the frequency characteristics of a climate control system based on thermoelectric Peltier modules.

Block diagram of the climate control system based on TEM

An example of a block diagram of a climate control system based on TEM is presented in Fig. 1. The features of this scheme in comparison with the known solutions are the presence of two temperature control channels, as well as the application of the combined control principle [27-30], which allows both a high speed of temperature transients and high interference suppression.

The diagram shows: TC1, 2–temperature control devices, TEM–termoelectric Peltier module, TD1,2–temperature detectors (sensors), Comp1,2–inertia compensators, WD–weight distributor (adder with variable weight coefficients), F and Amp – filter and amplifier; ϵ_{TC1} , ϵ_{TC2} and interference ϵ_{TEM} – factors affecting the corresponding blocks. The effects of ϵ_{TC1} , ϵ_{TC2} are determined by changes of the desired temperature at two points of the device, the output of the system is the temperature of a point source of heat or cold.

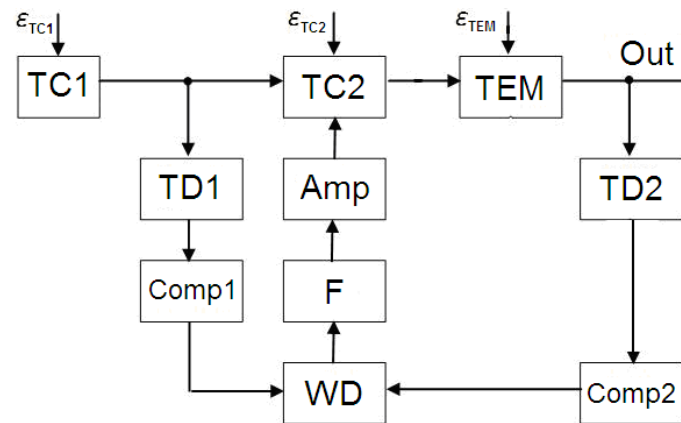


Fig. 1- Block diagram of a two-channel climate control system based on TEM with combined control

Transfer functions of the TEM-based climate control system

Let's denote the system parameters: n_{Amp} – the gain of the Amp, $M(p)$ – the transfer function of the filter, K with different lower indices-the transfer functions of the other blocks, $p=d/dt$ – the operator.

Taking into account the above designations, the transfer functions of the system take the form

$$\begin{aligned} H_{TC1}^{(\varepsilon)}(p) &= \frac{K_{TC1} + n_{Amp} K_{TC2} K_{WD1} K_{Comp1} K_{TD1} M(p)}{1 + n_{Amp} K_{TC2} K_{WD2} K_{Comp2} K_{TD2} M(p)}, \\ H_{TC2}^{(\varepsilon)}(p) &= \frac{K_{TC2}}{1 + n_{Amp} K_{TC2} K_{WD2} K_{Comp2} K_{TD2} M(p)}, \\ H_{TEM}^{(\varepsilon)}(p) &= \frac{K_{TEM}}{1 + n_{Amp} K_{TC2} K_{WD2} K_{Comp2} K_{TD2} M(p)}. \end{aligned} \quad (1)$$

The transfer functions fully describe the dynamic and selective properties of the climate control system at the linear mode. The transmission coefficient of the ventilation system connected at the TEM output can be easily taken into account in the TEM transfer function.

To normalize the transfer functions, we assume $K_{TC1} = K_{TC2} = K_{TEM} = 1$. Then, based on (1), the generalized transfer function for any of three influences effects takes the form

$$H_x(p) = \frac{q_x + \zeta_x N_c M(p)}{1 + N_c M(p)}, \quad (2)$$

where q_x , ζ_x are the coefficients of a specific transfer function, N_c – generalized control coefficient.

The frequency characteristics of the system are determined by the selective properties of the inertial links, which can be taken into account in the transfer function of the filter F, as well as in the coefficients of the formula (2). For arbitrary filter configurations, its transfer coefficient is conveniently represented by a fractional-rational function

$$M(p) = \frac{A(p)}{B(p)} = \frac{\sum_{i=0}^{\Psi} \alpha_i p^i}{\sum_{i=0}^{\Psi} \beta_i p^i}, \quad (3)$$

where Ψ is the order of the filter, α_i and β_i are the coefficients of the filter polynomials.

We substitute (3) into (2) and after the transformation obtain a generalized transfer function of the system with an arbitrary filter

$$H_x(p) = \frac{\mu_x(p)}{\nu_x(p)} = \frac{q_x B(p) + \zeta_x N_c A(p)}{B(p) + N_c A(p)}. \quad (4)$$

We replace $p \rightarrow j\Omega$, and then the ratio (4) turns into a complex fraction. We denote the real (*Re*) and imaginary (*Im*) components by the lower indices *R* and *I*. The ex-

pressions for the amplitude and phase frequency response characteristics (AFC and PFC) of the device are written as

$$K_X(\Omega) = |H_X(j\Omega)| = \sqrt{\frac{[\mu_{XR}(\Omega)]^2 + [\mu_{XI}(\Omega)]^2}{[\nu_{XR}(\Omega)]^2 + [\nu_{XI}(\Omega)]^2}},$$

$$\Phi_X(\Omega) = \arg[H_X(j\Omega)] = \arctg \frac{\mu_{XI}(\Omega)}{\mu_{XR}(\Omega)} - \arctg \frac{\nu_{XI}(\Omega)}{\nu_{XR}(\Omega)}, \quad (5)$$

where $\mu_{XR,I}(\Omega) = q_X B_{R,I}(\Omega) + \zeta_X N_C A_{R,I}(\Omega)$ and $\nu_{XR,I}(\Omega) = B_{R,I}(\Omega) + N_C A_{R,I}(\Omega)$ are the components of the numerator and denominator.

Taking into account the coefficients of the filter polynomials, the real and imaginary components of the transfer functions of the filter and the system as a whole take the form

$$A_R(\Omega) = \sum_{i=0}^{\lfloor \frac{\Psi}{4} \rfloor} \alpha_{4i} \Omega^{4i} - \alpha_{4i+2} \Omega^{4i+2},$$

$$B_R(\Omega) = \sum_{i=0}^{\lfloor \frac{\Psi}{4} \rfloor} \beta_{4i} \Omega^{4i} - \beta_{4i+2} \Omega^{4i+2},$$

$$\mu_{XR}(\Omega) = \sum_{i=0}^{\lfloor \frac{\Psi}{4} \rfloor} (q_X (\beta_{4i} \Omega^{4i} - \beta_{4i+2} \Omega^{4i+2}) + \zeta_X N_C (\alpha_{4i} \Omega^{4i} - \alpha_{4i+2} \Omega^{4i+2})),$$

$$\nu_{XR}(\Omega) = \sum_{i=0}^{\lfloor \frac{\Psi}{4} \rfloor} ((\beta_{4i} + N_C \alpha_{4i}) \Omega^{4i} - (\beta_{4i+2} + N_C \alpha_{4i+2}) \Omega^{4i+2});$$

$$A_I(\Omega) = \sum_{i=0}^{\lfloor \frac{\Psi}{4} \rfloor} \alpha_{4i+1} \Omega^{4i+1} - \alpha_{4i+3} \Omega^{4i+3},$$

$$B_I(\Omega) = \sum_{i=0}^{\lfloor \frac{\Psi}{4} \rfloor} \beta_{4i+1} \Omega^{4i+1} - \beta_{4i+3} \Omega^{4i+3},$$

$$\mu_{XI}(\Omega) = \sum_{i=0}^{\lfloor \frac{\Psi}{4} \rfloor} (q_X (\beta_{4i+1} \Omega^{4i+1} - \beta_{4i+3} \Omega^{4i+3}) + \zeta_X N_C (\alpha_{4i+1} \Omega^{4i+1} - \alpha_{4i+3} \Omega^{4i+3})),$$

$$\nu_{XI}(\Omega) = \sum_{i=0}^{\lfloor \frac{\Psi}{4} \rfloor} ((\beta_{4i+1} + N_C \alpha_{4i+1}) \Omega^{4i+1} - (\beta_{4i+3} + N_C \alpha_{4i+3}) \Omega^{4i+3}) \quad (6)$$

In expressions (6) the symbol $\lfloor \bullet \rfloor$ denotes the truncation to the nearest integer.

The analytical calculation of the frequency characteristics of the system can be per-

formed by the expression (5) by directly substituting the filter polynomials $A_{R,I}(\Omega)$, $B_{R,I}(\Omega)$ or their coefficients α_i and β_i into the system polynomials $\mu_{X,R,I}(\Omega)$ and $\nu_{X,R,I}(\Omega)$.

To suppress interference with different spectrum shapes, the system requires a filter with a complex selectivity characteristic. It can be represented by a cascade connection of various types of links. Filter transfer function

$$M(p) = \frac{A(p)}{B(p)} = \frac{\prod_{i=1}^{\Psi} (\zeta_{Fi} + m_i T_i p)}{\prod_{i=1}^{\Psi} (1 + T_i p)}, \tag{7}$$

where m_i is the proportionality coefficient of the i -th link: $m_i = 0$ for the low-pass filter (LPF) and $m_i = 0...1$ for the proportional-integrating filter (PIF); T_i is the time constant of the link number i , taking into account the influence of other links, the filter link type parameter $\zeta_{Fi}=1$ for the LPF link, $\zeta_{Fi}=0$ for the high-pass filter link (HPF). For brevity we denote $\zeta_{Fi} = \zeta$ (all filter links are of the same type).

We express the time constants T_i in terms of the time constant of the first link: $T_1=T$, $T_2=\lambda T$, $T_3=\gamma T$, and $T_4=\eta T$, where λ , γ , and η are the coefficients. Taking into account the accepted designations, the expressions for the coefficients and polynomials of the filter up to the 4th order take the form shown in Table 1, here $\hat{\Omega} = \Omega T$ is the normalized frequency.

As follows from (4) and (5), the filter coefficients β_i and the filter polynomials $B_{R,I}(\Omega)$ are determined by the table expressions by substitution $\zeta_{Fi}=\zeta=1$ and $m_i=m=1$.

Table 1- Coefficients and polynomials of the filter of the 1st-4th orders of the climate control system based on TEM

Filter order Ψ	Coefficients of the filter's numerator					Filter polynomials	
	a_0	a_1	a_2	a_3	a_4	Real $A_R(\hat{\Omega})$	Imaginary $A_I(\hat{\Omega})$
1	Z	m	0	0	0	ζ	$m \hat{\Omega}$
2	ζ^2	$\zeta(m_1+m_2\lambda)$	$m_1 m_2 \lambda$	0	0	$\zeta^2 - m_1 m_2 \lambda \hat{\Omega}^2$	$(m_1+m_2\lambda)\zeta \hat{\Omega}$
3	ζ^3	$\zeta^2(m_1+m_2\lambda+m_3\gamma)$	$\zeta(m_1 m_2 \lambda + m_1 m_3 \gamma + m_2 m_3 \lambda \gamma)$	$m_1 m_2 m_3 \lambda \gamma$	0	$\zeta^3 - (m_1 m_2 \lambda + m_1 m_3 \gamma + m_1 m_2 \lambda \gamma) \zeta \hat{\Omega}^2$	$(m_1+m_2\lambda+m_3\gamma)\zeta^2 \hat{\Omega} - m_1 m_2 \lambda \gamma \hat{\Omega}^3$
4	ζ^4	$\zeta^3(m_1+m_2\lambda+m_3\gamma+m_4\eta)$	$\zeta^2(m_1 m_2 \lambda + m_1 m_3 \gamma + m_1 m_4 \eta + m_2 m_3 \lambda \gamma + m_2 m_4 \lambda \eta + m_3 m_4 \gamma \eta)$	$m_1 m_2 m_3 \lambda \gamma + m_1 m_2 m_4 \lambda \eta + m_1 m_3 m_4 \gamma \eta + m_2 m_3 m_4 \lambda \gamma \eta$	$m_1 m_2 m_3 m_4 \lambda \gamma \eta$	$\zeta^4 - (m_1 m_2 \lambda + m_1 m_3 \gamma + m_1 m_4 \eta + m_2 m_3 \lambda \gamma + m_2 m_4 \lambda \eta + m_3 m_4 \gamma \eta) \zeta^2 \hat{\Omega}^2 + m_1 m_2 m_3 m_4 \lambda \gamma \eta \hat{\Omega}^4$	$(m_1+m_2\lambda+m_3\gamma)\zeta^3 \hat{\Omega} - (m_1 m_2 m_3 \lambda \gamma + m_1 m_2 m_4 \lambda \eta + m_1 m_3 m_4 \gamma \eta + m_2 m_3 m_4 \lambda \gamma \eta) \zeta \hat{\Omega}^3$

Frequency characteristics of the TEM-based climate control system

The frequency characteristics of the system are obtained by substituting tabular coefficients or polynomials in (6) and then in (5). Further, in the filter name, its order will be denoted by a digit after the filter name (for example, PIF1).

So, the frequency characteristics of the system with PIF1

$$K_{x_1}(\hat{\Omega}) = \sqrt{\frac{[q_x + \zeta_x N_c \zeta_F]^2 + (q_x + \zeta_x N_c m)^2 \hat{\Omega}^2}{[1 + N_c \zeta_F]^2 + (1 + N_c m)^2 \hat{\Omega}^2}},$$

$$\Phi_{x_1}(\hat{\Omega}) = \arctg \frac{(q_x - \zeta_x N_c m) \hat{\Omega}}{q_x - \zeta_x N_c \zeta_F} - \arctg \frac{(1 + N_c m) \hat{\Omega}}{1 + N_c \zeta_F}.$$

The characteristics of the system with PIF2 take the form

$$K_{x_2}(\hat{\Omega}) = \sqrt{\frac{[q_x(1 - \lambda \hat{\Omega}^2) + \zeta_x N_c (\zeta_F^2 - m_1 m_2 \lambda \hat{\Omega}^2)]^2 + \rightarrow}{[1 - \lambda \hat{\Omega}^2 + N_c (\zeta_F^2 - m_1 m_2 \lambda \hat{\Omega}^2)]^2 + \rightarrow}}$$

$$\rightarrow \frac{+ [q_x(1 + \lambda) \hat{\Omega} + \zeta_x N_c \zeta_F (m_1 + m_2 \lambda) \hat{\Omega}]^2}{+ [(1 + \lambda) \hat{\Omega} + N_c \zeta_F (m_1 + m_2 \lambda) \hat{\Omega}]^2},$$

$$\Phi_{x_2}(\hat{\Omega}) = \arctg \frac{q_x(1 + \lambda) \hat{\Omega} + \zeta_x N_c \zeta_F (m_1 + m_2 \lambda) \hat{\Omega}}{q_x(1 - \lambda \hat{\Omega}^2) + \zeta_x N_c (\zeta_F^2 - m_1 m_2 \lambda \hat{\Omega}^2)} -$$

$$- \arctg \frac{(1 + \lambda) \hat{\Omega} + N_c \zeta_F (m_1 + m_2 \lambda) \hat{\Omega}}{1 - \lambda \hat{\Omega}^2 + N_c (\zeta_F^2 - m_1 m_2 \lambda \hat{\Omega}^2)}. \quad (8)$$

Characteristics of the system with LPF3

$$K_{x_3}(\hat{\Omega}) = \sqrt{\frac{\{q_x [1 - (\lambda + \gamma + \lambda \gamma) \hat{\Omega}^2] + \zeta_x N_c\}^2 + \rightarrow}{[1 - (\lambda + \gamma + \lambda \gamma) \hat{\Omega}^2 + N_c]^2 + \rightarrow}}$$

$$\rightarrow \frac{+ q_x^2 [(1 + \lambda + \gamma) \hat{\Omega} - (\lambda \gamma) \hat{\Omega}^3]^2}{+ [(1 + \lambda + \gamma) \hat{\Omega} - \lambda \gamma \hat{\Omega}^3]^2}.$$

$$\Phi_{x_3}(\hat{\Omega}) = \arctg \frac{q_x^2 [(1 + \lambda + \gamma) \hat{\Omega} - (\lambda \gamma) \hat{\Omega}^3]}{q_x [1 - (\lambda + \gamma + \lambda \gamma) \hat{\Omega}^2] + \zeta_x N_c} -$$

$$- \arctg \frac{(1 + \lambda + \gamma) \hat{\Omega} - (\lambda \gamma) \hat{\Omega}^3}{1 - (\lambda + \gamma + \lambda \gamma) \hat{\Omega}^2 + N_c}. \quad (9)$$

Simulation results

Graphs of the frequency characteristics of a system with different types of filters under influence ε_{TC2} are shown in Fig. 2, 3, and 4. Influence parameters are $q_X = q_{TC2}^{(\varepsilon)} = -1$, filter coefficients are $\lambda=3, \gamma=2, \eta=1$.

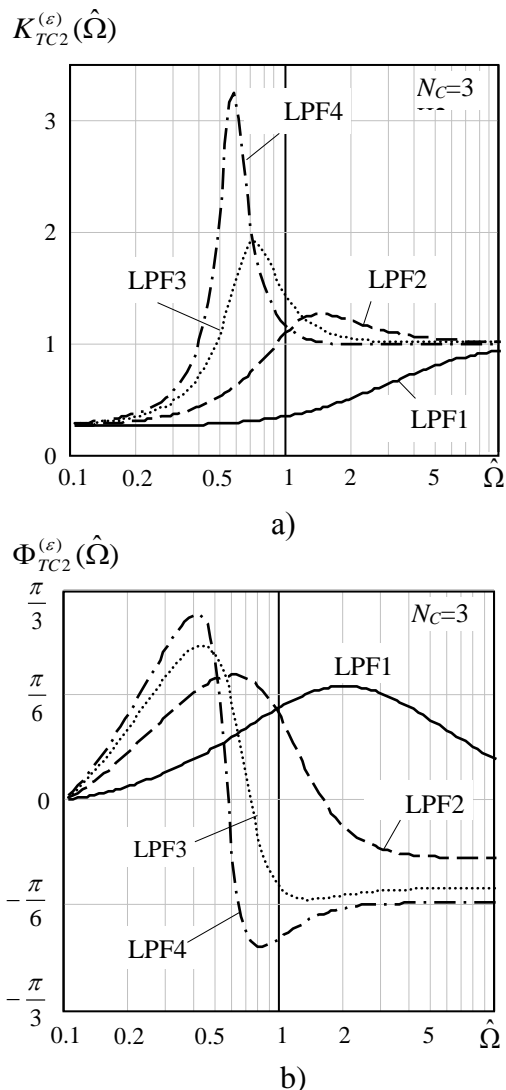


Fig. 2 – Amplitude-frequency (a) and phase-frequency (b) characteristics of the climate control system with low-pass filters of the 1st-4th orders

The frequency response of a system with LPF1 (Fig. 2a) is a monotone function of frequency. With an increase in the filter order, the nonlinearity of both frequency characteristics increases, and the frequency response of the system (Fig. 1b) acquires an extremum. The frequency response extremum increases and shifts to the left along the frequency axis, the PFC value $\Phi_{TC2}^{(\varepsilon)}(\infty)$ decreases.

For a device with LF3 (Fig. 3), the static compensation error $K_{TC2}^{(\varepsilon)}(0)$ decreases with increasing N_C , the nonlinearity of the AFC and PFC increases, the extremum of AFC shifts to the left and increases, reaching a maximum at $N_C=10$.

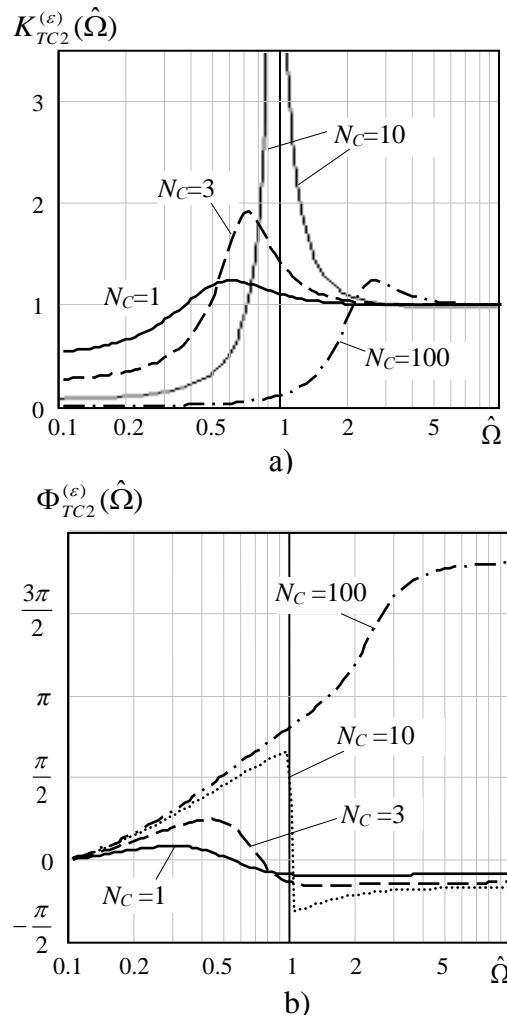


Fig. 3- Amplitude-frequency (a) and phase-frequency (b) characteristics of a climate control system with a 3rd order low-pass filter for various gain coefficients N_C

For a system with PIF3 (Fig. 4), with an increase of m from 0 to 0.15, the extremal value of the AFC decreases. With a further growth of m from 0.3 to 0.5, the AFC becomes monotonous and the transmission coefficient of the system $K_{TC2}^{(\varepsilon)}(\infty)$ decreases. At an optimal value of m the frequency characteristics become steeper and the APC extremal value grows.

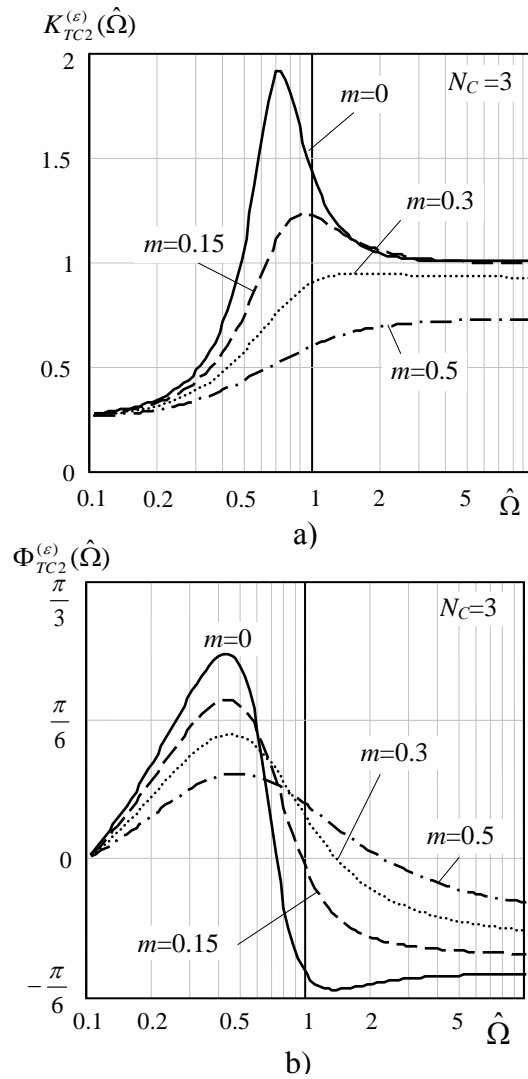


Fig. 4- Amplitude-frequency (a) and phase-frequency (b) characteristics of a climate control system with a 3rd order PIF for various proportionality coefficients m

Conclusion

In order to achieve a high accuracy of temperature control by changing the power supply current, it is necessary to develop an effective control system for thermoelectric modules (TEM). A climate control system based on TEM and the principle of combined control with improved dynamic and noise-resistant properties compared to known solutions has been developed. Analytical expressions are obtained and graphs of the frequency characteristics of the system are developed for various types and orders of the filter in the control circuit (integrating and proportionally integrating low-pass filters from the 1st to the 4th orders). The conducted studies allow us to select the parameters of the climate control system blocks to obtain the desired laws of tempera-

ture change and reduce the influence of destabilizing factors.

Acknowledgements

The article was prepared as part of the state task "Research and development of complex energy-saving and thermoelectric regenerative systems" application number 2019-1497, subject number FZWG-2020-0034.

Reference

- [1] Galimova L. V., Slavin R. B. Analysis of the efficiency of an energy-saving trigeneration system / Refrigeration equipment - No. 3. - 2012. - p. 16-19.
- [2] Wang, J.; Wu, J.; Zheng, C. (2014): Analysis of trigeneration system in combined cooling and heating mode. *Energy and Buildings*, 72, pp. 353–360.
- [3] Wei He, Jinzhi Zhou, Jingxin Hou, Chi Chen, Jie Ji 2013, Theoretical and experimental investigation on a thermoelectric cooling and heating system driven by solar, *Applied Energy* 107 - 89-97.
- [4] Thermoelectric Module Market Expected to Reach US\$ 1,713.9 Mn by 2027: Transparency Market Research: <https://www.transparencymarketresearch.com/pressrelease/thermoelectric-modules-market.htm>
- [5] Shostakovskiy P. Modern solutions of thermoelectric cooling for radioelectronic, medical, industrial and household appliances // *Components and technologies*. 2009. № 12. 2010. № 1.
- [6] Frolov S. S., Kulsarin A. A. Method for determining the characteristics of a Peltier element for dry-air temperature control of a quartz capillary of a capillary electrophoresis system No. 5, 2018.
- [7] Christian J.L. Hermes, Jader R. Barbosa Jr., Thermodynamic comparison of Peltier, Stirling, and vapor compression portable coolers, *Appl. Energy* 91 (2012) 51-58.
- [8] D. Reid, Food preservation, *ASHRAE J.* 41 (1999) 40-45.
- [9] D. Astrain, A. Martinez, A. Rodriguez, Improvement of a thermoelectric and vapour compression hybrid refrigerator, *Appl. Therm. Eng.* 39 (2012) 140-150.
- [10] Suwit Jugsujinda, et al., Analyzing of thermoelectric refrigerator performance, *Procedia Eng.* 8 (2011) 154-159.
- [11] Jihui Yang, F.R. Stabler, Automotive applications of thermoelectric materials, *J. Electron. Mater.* 38 (7) (2009).

- [12] S.B. Riffat, Guoquan Qiu, Comparative investigation of thermoelectric air-conditioners versus vapour compression and absorption air-conditioners, *Appl. Therm. Eng.* 24 (2004) 1979-1993
- [13] Yu-Wei Chang, Chih-Chung Chang, Ming-Tsun Ke, Sih-Li Chen, Thermoelectric air-cooling module for electronic devices, *Appl. Therm. Eng.* 29 (2009) 2731-2737.
- [14] M.A. Ahamat, M.J. Tierney, Timewise temperature control with heat metering using a thermoelectric module, *Appl. Therm. Eng.* 31 (2011) 1421-1426.
- [15] Lon E. Bell et al., High capacity thermoelectric temperature control system, United States Patent, 7946120B2, May 24, 2011
- [16] Zhong Bing Liu, Ling Zhang, GuangCai Gong, YongQiang Luo, FangFang Meng Experimental study and performance analysis of a solarthermoelectric air conditioner with hot water supply. *Energy and Buildings* 86 (2015) 619–625.
- [17] Yazeed Alomair, Muath Alomair, Shohel Mahmud. 2015 Theoretical and Experimental Analyses of Solar-Thermoelectric Liquid-Chiller System *International Journal of Refrigeration*, doi: 10.1016/j.ijrefrig.2015.01.003
- [18] M.Aboelmaaref, Moustafa & Askalany, Ahmed & Harbi, Khalid. (2017). Solar thermoelectric cooling technology
- [19] Guiatni, Mohamed & Drif, Abdelhamid & Kheddar, Abderrahmane. (2007). Thermoelectric Modules: Recursive non-linear ARMA modeling, Identification and Robust Control. 568 - 573. DOI: 10.1109/IECON.2007.4460142.
- [20] Guiatni, Mohamed & Kheddar, Abderrahmane. (2011). Modeling Identification and Control of Peltier Thermoelectric Modules for Telepresence. *Journal of Dynamic Systems, Measurement, and Control.* 133. 031010. 10.1115/1.4003381.
- [21] Photoon, Rung-aroon & Wichakool, Warit. (2015). System identification of Thermoelectric generator using a first order plus dead time model. 1-5. DOI: 10.1109/ECTICon.2015.7207047.
- [22] Vasilyev, G.S., Kuzichkin, O.R., Surzhik, D.I. Method for modeling dynamic modes of nonlinear control systems for thermoelectric modules (2021) *Advances in Dynamical Systems and Applications*, 15 (2), pp. 187-197. DOI: 10.37622/ADSA/15.2.2020.187-197.
- [23] Surzhik, D.I., Kuzichkin, O.R., Vasilyev, G.S. An integrated approach to the construction of energy-saving trigeneration systems for objects of the agro-industrial complex (2021) *International Journal of Engineering Research and Technology*, 13 (12), pp. 4622-4626.
- [24] Grinkevich V. A. Synthesis of the current controller for Peltier element // *Collection of scientific works NSTU.* – 2018. – No 3-4 (93). – P. 16-39. – DOI: 10.17212/2307-6879-2018-3-4-16-39.

- [25] Grinkevich V. A. Investigation of a mathematical model of a thermostat based on the Peltier element / Collection of scientific works of NSTU. – 2017. – No 3 (89). – Pp. 62-77.
- [26] Grinkevich V. A. Synthesis of a temperature controller for Peltier element // Collection of scientific works NSTU. – 2019. – No 1 (94). – P. 7-31. – DOI: 10.17212/2307-6879-2019-1-7-31.
- [27] Esakov V. F. et al. Automatic gain control in low-frequency amplifiers. - Moscow: Energiya, 1970 – 80 p.
- [28] Vasilyev, G.S., Kuzichkin, O.R., Kurilov, I.A., Surzhik, D.I. Analysis of noise properties of hybrid frequency synthesizer with autocompensating phase noise of DDS and PLL (2016) 2016 International Siberian Conference on Control and Communications, SIBCON 2016 - Proceedings, статья № 7491742, . DOI: 10.1109/SIBCON.2016.7491742
- [29] Kurilov, I.A. Research of static characteristics of converters of signals with a nonlinear control device / I.A. Kurilov, G.S. Vasilyev, S.M. Kharchuk, D.I. Surzhik // 2011 International Siberian Conference on Control and Communications (SIBCON)/ Proceedings. – Krasnoyarsk: Siberian Federal University. Russia, Krasnoyarsk, September 15-16, 2011. – p. 93 – 96. IEEE Catalog Number: CFP13794-CDR, IEEEXplore, <http://conf.sfu-kras.ru/conf/sibcon> ISBN: 978-1-4577-1069-8/11/2011 IEEE.
- [30] Vasilyev, G.S., Surzhik, D.I., Kuzichkin, O.R., Bondarik, K.V. Hierarchical model of information signals formation at the physical layer in FANET (2020) 7th International Conference on Control, Decision and Information Technologies, CoDIT 2020, статья № 9263959, pp. 1221-1225. DOI: 10.1109/CoDIT49905.2020.9263959

